Nuclear Instruments and Methods in Physics Research A 809 (2016) 130–139

Contents lists available at ScienceDirect

Nuclear Instruments and Methods in Physics Research A

journal homepage: www.elsevier.com/locate/nima

Development of new scintillators for medical applications

Paul Lecoq *

CERN, Route de Meyrin, 1211 Geneva, Switzerland

ARTICLE INFO

Available online 2 September 2015

Keywords:
Crystal
Scintillator
Medical imaging
PET
SPECT

ABSTRACT

For a long time the discovery of new scintillators has been more serendipitous than driven by a deep understanding of the mechanisms at the origin of the scintillation process. This situation has dramatically changed since the 1990's with an increased demand for scintillators of better performance for large particle physics experiments as well as for medical imaging. It is now possible to design a scintillator for a specific purpose. The bandgap can be adjusted, the traps energy levels and their concentration can be finely tuned and their influence can be damped or on the contrary enhanced by specific doping for an optimization of the performance of the scintillator. Several examples are given in this paper of such crystal engineering attempts to improve the performance of crystal scintillators used in medical imaging devices.

An attention is also given to spectacular progress in crystal production technologies, which open new perspectives for large scale and cost effective crystal production with consistent quality.

1. Introduction

In the current clinical practice medical imaging is aiming at the in-vivo anatomic and functional visualization of organs in a non- or minimally invasive way. X-ray imaging is the historical imaging modality since the discovery of X-rays and the pioneering work of W. Roentgen in 1895. Since that time it remains the most widely used imaging diagnosis tool for physicians with nearly half a billion X-ray exams performed every year worldwide. Besides direct conversion detectors like amorphous Silicon, CdTe or CdZnTe scintillation materials are still the detectors of choice for modern X-ray detectors.

More recently isotopic imaging, in particular PET, has seen a spectacular development because of its very high sensitivity at the picomolar level, allowing in-vivo molecular-imaging-based investigations of biochemical pathways and precision diagnostics. Isotopic imaging consists in injecting into a patient a molecule involved in a specific metabolic function so that this molecule will preferentially be fixed on the organs or tumors where the function is at work. The molecule has been labeled beforehand with a radioisotope emitting gamma photons like ^{99}Tc (Single Photon Emission Computed Tomography or SPECT) or with a positron-emitting isotope like ^{18}F, ^{11}C, ^{15}O, ^{13}N (Positron Emission Tomography or PET). In the latter case, the positron annihilates very quickly on contact with ordinary matter, emitting two gamma photons located on the same axis called the line of response (LOR) but in opposite directions with a precise energy of 511 keV each. Analyzing enough of these gamma photons, either single for SPECT or in pairs for PET makes it possible to reconstruct the image of the areas (organs, tumors) where the tracer focused.

The scintillating crystals are the eyes of PET and SPECT scanners as they provide the relevant information about each gamma event, i.e. the exact position and time of its conversion in the detector and its energy.

2. Scintillator requirements

The required performance of radiation detectors used in X-ray and nuclear medicine imaging devices is related to the detection efficiency and the precise determination of the position, the emission time and the energy of X-rays and gamma rays involved in these imaging modalities. These requirements are therefore dependant on the energy of the photons to be detected, which ranges from a few tens of keV for soft X-ray imaging up to 511 keV for PET scanners.

2.1. X-ray imaging

Modern digital radiography devices and CT scanners use scintillator material arrays optically coupled to matching silicon p–i–n photodiode matrices. The patient radiation exposure being an important issue the scintillating material must be dense enough to absorb close to 100% of the impinging X-rays, thus minimizing the

* Tel.: +41 75 411 0268; fax: +41 22 767 8930.
E-mail address: paul.lecoq@cern.ch

http://dx.doi.org/10.1016/j.nima.2015.08.041

patient dose required for a given image quality. Ceramic phosphors are commonly used for thin scintillation screens (0.1 mm to 0.2 mm thickness), which are well adapted to the lowest X-ray energies (for instance about 20 keV for X-ray mammography), because they can be produced in any shape at a reasonable cost. On the other hand for dental X-ray diagnostics (about 60 keV) and full body X-ray computed tomography (up to 150 keV) the required stopping power imposes much thicker screens and monocrystalline inorganic scintillators have been generally preferred up to now because of their much higher light transparency than ceramics. However recent progress in the production of nano-powders with low dispersion grain diameter have paved the way for manufacturing more transparent ceramics.

Latest generation X-ray CT scanners are recording about 1000 projections (subject slices) per second. This imposes severe constrains on both the decay time and afterglow of the scintillating material. Afterglow is known to produce ghost images through a "memory effect" which deteriorates the quality of the images.

The requirements for the scintillator material to be used in X-ray CT can be summarized as follows:

- High absorption for X-rays in the energy range up to 150 keV. An absorption coefficient close to 100% for $\sim$2 mm thick material layer is required. This characteristic is directly related to the X-ray CT image noise. Indeed the image quality is limited in low contrast regions by statistical fluctuations in the numbers of detected X-rays. A high detection efficiency allows to keep the patient dose exposure within reasonable limits for a given image quality.

- High light output, typically of the order or greater than 20,000 photons/MeV in order to reduce the image noise at low signal levels.
- Radioluminescence spectrum in the visible, or near IR range to match the spectral sensitivity of the silicon photodetectors.
- Decay time in the range of 1–10 μs, in order to match the sampling rates of the CT scanners in the $\geq$10 kHz range.
- No afterglow. This is the most severe constraint. Afterglow is generally caused by material imperfections (impurities, defects), causing delayed thermally assisted release of trapped charge carriers and their recombination with decay times in the range 100 ms to 10 s. An afterglow level of less than 0.1% is generally required 3 ms after the end of a continuous X-ray excitation. Afterglow causes sickle artifacts in the CT images.
- Good radiation hardness for high X-ray fluence. The integrated exposure of the scintillators can reach several tens of kGy over the lifetime of a CT scanner. Changes in the light yield cause detector gain instability, resulting in ring image artifacts. Long-term changes of $\sim$10% are acceptable, while only less than 0.1% short term changes during the daily operation (10 Gy) can be tolerated without image quality degradation.
- Small temperature dependence of the light yield. The X-ray generation system usually dissipates a high amount of energy and the temperature of the detectors can change rapidly. A light output temperature coefficient within $\pm$0.1%/°C is desirable, which is a rather stringent requirement. It is related to the probability of non-radiative transitions and expressed by Mott's equation:

$$I(T) \approx \left(1 + \omega_0 \exp(-\varepsilon/kT)\right)^{-1}$$

- In the case of Cadmium Tungstate (the most frequently used crystal in modern commercial CT scanners) the frequency factor $\omega_0 = 4.25 \times 10^6$ and the thermal activation energy $\varepsilon = 0.49$ eV [1], resulting in an acceptable temperature coefficient of $-0.3\%/°C$.
- Good mechanical properties allowing micromachining of 2D scintillator arrays with pixel dimensions less than 1 mm.
- Affordable cost.

2.2. PET and SPECT

The challenge for functional isotopic imaging lays in its capacity to quantitatively measure the relative metabolic activity of the specific molecular pathways in action in a metabolic process. To achieve this it is necessary to improve both the imaging system's spatial resolution, that is, its capacity to discriminate two separate objects. An important point is to achieve a good image signal to noise ratio in order to precisely evaluate a metabolic agent's concentration in an organ or group of cells. The precision of the concentration's measurement depends mainly, but not only, on the imaging system's sensitivity, and therefore its capacity to accumulate the statistics needed to reconstruct in-vivo the 4D (space and time) distribution of the radiopharmaceutical.

The focus put on personalized medicine as one priority of modern healthcare challenges isotopic imaging for increased performance towards molecular imaging with specific requirements on:

- improving detector sensitivity
- improving spatial resolution
- improving energy resolution
- improving temporal resolution

This imposes a serious effort in improving the performance of each component of the whole detection chain as well as in data processing and image reconstruction algorithms.

At the level of scintillator materials the first important requirement is the stopping power for the given energy range of X and γ rays to be considered, and more precisely the conversion efficiency. Clearly materials with high Z and high density are favored but the position of the K-edge is also important as can be seen in Fig. 1. If for low energy X-ray imaging (below 63 keV) the attenuation coefficient of Yttrium, Caesium and Iodine are quite high and crystals like YAP and CsI are good candidates, above the K-edge of Lu (63 keV) and Bismuth (90 keV) the situation is quite different and BGO and Luthetium based crystals will be clearly favored for ^{99}Tc (140 keV) SPECT and PET scanners. (511 keV). Heavy scintillators are also useful to reduce their thickness and consequently the parallaxial error in small diameter ring imagers.

A high light yield is also mandatory to improve the energy resolution, which is essentially limited by the photo statistics and the electronic noise at these energies. A better energy resolution allows a higher rejection of tissue-scattered events and Compton

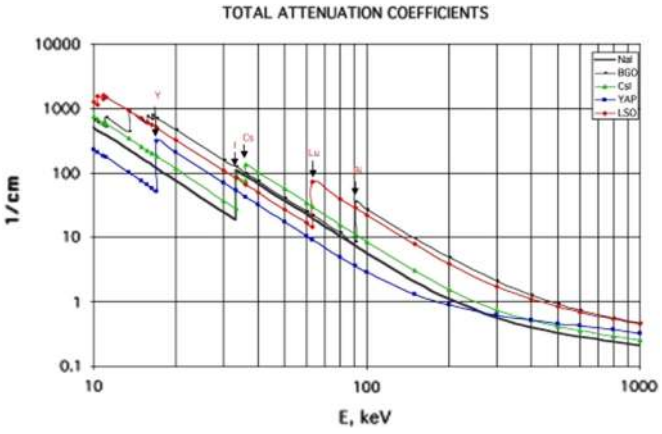

Fig. 1. Attenuation coefficient in several high Z materials.

events in the crystals and improves therefore the spatial resolution and the sensitivity. The sensitivity is a very critical parameter of nuclear medical imaging as it reflects the number of useful events per unit of injected dose to the patient. A higher sensitivity means a smaller injected dose or a better image contrast.

A short scintillation decay time allows to reduce the dead time and therefore to increase the limiting counting rate. Moreover by reducing the coincidence gate the signal to background ration is improved which has a direct impact on the image quality. Here again the sensitivity and image contrast are increased for a given patient dose, or the dose can be reduced. A particular attention is given these days to time-of- flight (TOF) PET scanners. Introducing TOF techniques allows improving the signal-to-noise ratio in PET images and reduces artifacts in case of partial ring configurations and incomplete tomographic reconstruction. Commercial PET scanners achieve about 600 ps FWHM coincidence time resolution (CTR) in the difference of detection time of the two 511 keV gamma rays resulting from the positron annihilation. This allows a significant image quality improvement particularly for overweighted patients. Ideally one would like to achieve 100 ps FWHM CTR resolution, which would correspond to a centimeter resolution along the LOR corresponding to the coincidence detection of the 2 gamma rays.

In first approximation (providing the detection threshold and the single photon response of the photodetector can be made small enough) the CTR for practical scintillators characterized by a scintillator rise time τ_r and a decay time τ_d is given by the following formula [2]:

$$\mathrm{CTR} \propto \sqrt{\frac{\tau_r \tau_d}{N_{phe}}}$$

where N_{phe} is the number of photoelectrons readout from the crystal, therefore directly related to the scintillator light yield. Improving the CTR implies increasing the photon rate in the leading edge of the scintillation pulse and requires a high light yield as well as a short rise time and decay time.

3. State of the art

3.1. X-ray imaging

The only crystalline material still in use in medical and security systems CT scanners is Cadmium Tungstate, $CdWO_4$, also called CWO. Its main advantage over CsI(Tl) is a very low afterglow level of 0.05% 3 ms after the end of the X-ray exposure and a reasonable temperature coefficient of 0.3%/°C. In spite of their wide use CWO crystals are however not optimal for CT applications due to their brittleness and the toxicity of Cadmium. Moreover it is difficult to manufacture crystals with adequate uniformity. This has been an argument for the search of a new generation of CT scintillators. This search was initiated by General Electric and Siemens in the mid of 80th when they introduced the first polycrystalline ceramic scintillators. The host materials are Yttrium and Gadolinum oxydes: Y_2O_3 and Gd_2O_3, which, after doping with Pr and Tb, demonstrate reasonable scintillation properties. However their transmission is rather low, ceramics being more translucent than transparent. The additional Eu^{3+} activator efficiently traps electrons to form a transient Eu^{2+} state, allowing holes to form Pr^{4+} and Tb^{4+} and, therefore, competes with the intrinsic traps responsible for afterglow. This energy trapped on the Pr and Tb sites decays non-radiatively in presence of the Eu ions reducing therefore the level of afterglow [3].

The historical Gadolinium oxyde ceramic is now replaced by yttrium gadolinum oxyde YGO [4], and gadolinum silicate GOS based ceramic materials [5]. When coupled to a silicon p–i–n photodiode they generate about 20 electrons per 1 keV of absorbed X-ray energy. However the long decay time of YGO (~1 ms) is a major concern and requires a complex algorithm of data deconvolution to suppress the effects of afterglow at the price of increased projection noise. Other ceramic materials proposed for CT applications are gadolinium gallium garnet, and lanthanum hafnate [6]. While ceramic materials are generally preferred to crystals because of their good performance and easy production in a variety of shapes, their low transparency requires the use of thin scintillators elements, with lower than optimal X-ray efficiency.

For the specific application domain of digital radiography a large R&D effort has been made by several companies to produce flat panels, where the standard scintillating crystal or ceramic pixels are replaced by detector arrays made of CsI(Tl) needles or small crystals (for example calcium tungstate CWO or YAP) directly coupled to photodiode arrays or segmented photomultipliers.

The main characteristics of the scintillators used in medical CT imaging are summarized in Table 1:

3.2. PET and SPECT

Although there is a trend for going to direct conversion materials like GaAs, CdZnTe (CZT) and CdTe, particularly for small animal imaging devices, the majority of SPECT scanners (also called scintigraphy camera) are still using NaI:Tl and CsI:Tl crystals. The performance of these crystals is adequate for SPECT imaging (see Table 2) but the main argument for their choice is related to the maturity in their production technology. Very large ingots of several hundreds of kilograms can be grown with consistent high quality allowing the production of the large slabs needed for the SPECT detector head. Moreover the mechanical processing of these crystals is relatively easy and well optimized and the moderate hygroscopicity is not a too severe problem to deal with. As a result the cost is well understood and reasonable.

For PET scanners BGO crystal arrays have been the first choice until the end of the nineties. The main advantage was the high density (7.1 g/cm^3) with the highest atomic number known for a scintillator (75), resulting in a high photoelectric conversion

Table 1
Properties of scintillators used in X-ray CT imaging.

Scintillator	Density (g/cm^3)	Thickness to stop 99% of 140 keV X-rays (mm)	Light yield (ph/MeV)/ temperature coëfficiënt (%/°C)	Peak of emission band (nm)	Primary decay time (μs)	Afterglow (% at 3 ms)
CsI(Tl)	4.52	6.1	54,000/0.02	550	1	0.5
$CdWO_4$ (CWO)	7.9	2.6	28,000/−0.3	495	2, 15	0.05
Gd_2O_3:Eu^{+3}	7.55	2.6	–	610	–	–
$(Y,Gd)_2O_3$:Eu,Pr,Tb (YGO)	5.9	6.1	42,000/0.04	610	1000	5
Gd_2O_2S:Pr,Ce,F (GOS)	7.34	2.9	50,000/−0.6	520	2.4	<0.1
Gd_2O_2S:Tb(Ce) (GOS)	7.34	2.9	50,000/−0.6	550	600	0.6
La_2HfO_7:Ti	7.9	2.8	13,000/–	475	10	–
$Gd_3Ga_5O_{12}$:Cr,Ce	7.09	4.5	39,000/–	730	150	<0.1

Table 2
Scintillators already used or in development for medical imaging. Particularly attractive parameters are marked in bold.

Scintillator	Type	Density (g/cm^3)	Light yield (Ph/MeV)	Emission wavelength (nm)	Decay time (ns)	Hygroscopic
NaI:Tl	Crystal	3.67	38,000	415	230	Yes
CsI:Tl	Crystal	4.51	**54,000**	550	1000	Slightly
BGO	Crystal	**7.13**	9000	480	300	No
GSO:Ce	Crystal	6.7	12,500	440	60	No
LSO:Ce	Crystal	**7.4**	**27,000**	420	**40**	No
LuAP:Ce	Crystal	**8.34**	10,000	365	**17**	No
$LaBr_3$:Ce	Crystal	5.29	**61,000**	358	35	Very

efficiency. Their main flaw is a slow decay time (300 ns) of the scintillating light. As a result, these scanners work with a limited sensitivity of about 1000 kcps/mCi/ml with a coincidence window of about 10 to 12 ns and a proportion of diffused events of more than 30%.

A new generation of scanners appeared in the years 2000 with crystals about 10 times faster than BGO and capability of determining interaction depth in the crystals thanks to phoswich technology or double readout schemes. A gain in sensitivity by about one order of magnitude and in spatial resolution by a factor 2 or 3 was expected, on condition that readout electronics adapted to these new performances could be simultaneously developed.

During these years, many groups, among which the Crystal Clear collaboration [7] have spent many efforts for pluri-disciplinary work involving experts in various aspects of materials sciences – crystallography, solid state physics, luminescence, photonics, defects in solids – as well as industries, in order to develop or better understand and improve the properties of new scintillating materials adapted to the demand for increasingly efficient detectors in physics and medical imaging.

Among these crystals Cerium doped Lutetium ortho-silicate (LSO) has been extensively studied since its discovery in 1990 and has become the crystal of choice for replacing BGO in PET scanners [8]. The majority of modern PET scanners are now based on LSO or its derivates. The main reason is a fast decay time of 40 ns and a light yield approaching 30,000 ph/MeV.

Other innovating crystals, such as those from the family of Lutetium perovskites (LuAP) [9] have been developed and are now being produced industrially. Their properties are similar to, and complementary to those of LSO (Lutetium oxyorthosilicate), which has replaced BGO in a new generation of PET scanners. LuAP can be used alone, or it can be combined in a particularly optimal way with LSO to determine the interaction depth in a detector head with a phoswich configuration LSO-LuAP. LuAP is attractive for PET applications because of its high – and unmatched to this day – density of 8.34 g/cm^3 and of its response time (17 ns), which is twenty times faster than BGO, and even twice faster than LSO. Although its light yield is about twice weaker than LSO, the linearity of its response as a function of energy is much superior, which results in an energy resolution at least equivalent to, if not better than, LSO.

At the same time Cerium doped Gadolinum ortho-silicate (GSO) has been developed as well as mixed Lutetium and Gadolinum ortho-silicate (LGSO) [10]. The variable decay time of these crystals as a function of Cerium concentration opens the possibility to use also two varieties of them or one of them in combination with LSO or LYSO in a phoswich to determine the depth of gamma ray interaction on the basis of pulse shape analysis [11].

The most attractive scintillating crystals currently available or being developed for nuclear medicine are presented in Table 2.

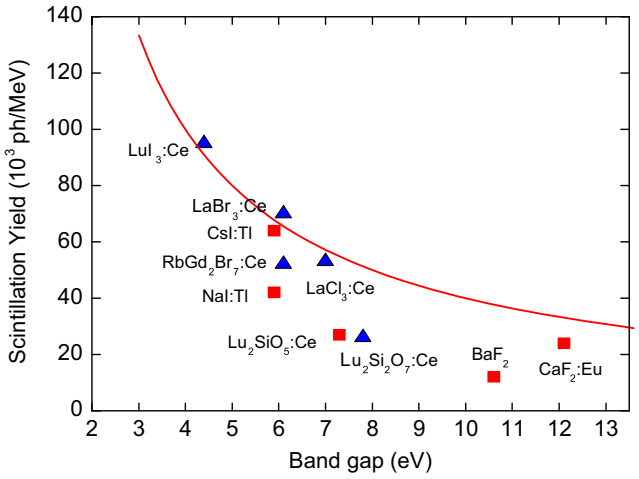

Fig. 2. Absolute photon yield of several scintillators as a function of the width of the forbidden band (Courtesy P. Dorenbos).

4. Fudamental limitations

4.1. Light yield

Light yield (LY) is an essential parameter for a scintillator as it directly influences the energy resolution at low or medium energy through the photostatistic term proportional to $(LY)^{-1/2}$ and the timing resolution proportional to $(\tau_{sc}/LY)^{-1/2}$, with τ_{sc} being the scintillation decay time. The scintillation mechanism is a several steps process and the overall scintillation yield is determined by the product of efficiencies for all these steps. The dominant factor, which sets the fundamental limit on the light output of a given scintillator, is the number n_{eh} of thermalized electron–hole pairs (active for scintillation) created by the interaction of ionizing radiation with the crystal:

$$n_{eh} = \frac{E_\gamma}{\beta \cdot E_g}$$

where $\beta \cdot E_g$ is the mean energy necessary for the formation of one thermalized electron–hole pair in a medium with a forbidden zone of width E_g and E_γ is the absorbed energy. For ionic crystals the factor β is usually close to 2.3 and takes into account the energy loss through coupling with lattice phonons during the thermalization process. As shown on Fig. 2 low bandgap materials are clearly better placed for high scintillation yield, although such materials are potentially more subject to trap induced quenching, re-absorption phenomena and photo-ionization of the luminescence center, which in turn will reduce this yield. The ultimate light yield obtained for a material having a bandgap of 3 eV and an emission wavelength of about 600 nm is in the range of 140,000 photons/MeV. The practical signal in photo-electrons/MeV is usually much smaller, as it has to account for a number of

losses in the conversion of the electron–hole pair into a photon, in the light transport to the photodetector and in the quantum efficiency of the photodetector.

4.2. Energy resolution, non-proportionality

The energy resolution is driven by several factors but two important parameters are playing an essential role. The first one is the light yield. The energy resolution is statistically determined by the number of photoelectrons produced in the photodetector, which is directly proportional to the number of photons extracted from the crystal. Therefore a high light yield will improve this statistical factor like $(n_{ph})^{-1/2}$.

The second factor is related to deviations from the linearity of response at low energy. Besides the well known peaks in the electron interaction cross-section near the K and L shells energy some crystals exhibit a non-proportionality behavior for excitations below 100 keV. The light yield can either increase when the excitation energy decreases, as is the case for halide crystals, or decrease, as for the majority of oxydes and fluorides. A few crystals only have response close to linear down to about 10 keV such as $YAlO_3$ (YAP), $LuAlO_3$ (LuAP), $LuYAlO_3$ (LuYAP), $LaBr_3$. Because of the balance between photoelectric, Compton scattering and pair production mechanism, the same total energy deposit in a crystal detector might result from the sum of contributions at different energies. The non-linearity affects therefore the energy resolution, as it is clearly illustrated by the examples of Lutetium orthosilicate (LSO) and Lutetium Aluminum Perovskite (LuYAP). For the same detector volume, LuYAP achieves similar energy resolution (9% @511 keV) than LSO despite a 3 times lower light yield [11], as a result of a more linear response at low energy, as shown in Fig. 3.

The main reason for this non-uniformity is related to the nature of the energy deposition of ionizing particles in the crystal, leading to a non-uniform density of ionization along their track [13]. High ionization density regions make possible interactions between charge carriers, excitons and excited ions or complex excited molecular structures in the crystal. Non-radiative relaxations are therefore possible, or on the contrary, new radiative channels from complex molecular excited systems, leading to quenching or light enhancing mechanisms and causing non-proportional responses at low energy. The charge carrier mobility in the host lattice plays an important role. A good understanding of these phenomena opens the possibility to tune it by proper co-doping and to improve the proportionality of the response and consequently the energy resolution. This has been demonstrated on strontium doped lanthanum halides [14].

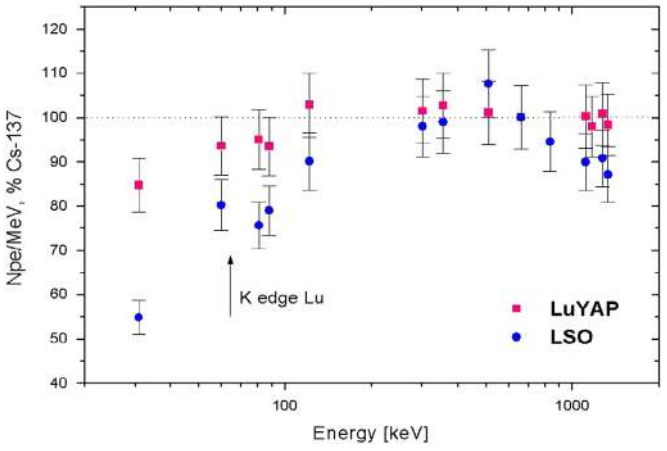

Fig. 3. Low energy response non-linearity for LSO and LuYAP crystals. From Ref. [12].

5. Future trends

Over the last 20 years several large projects in particle physics as well as the increasing demand for large quantities of scintillators with ever better performance for medical imaging and other applications has led the pluri-disciplinary community of experts working on scintillators to get organized and to structure the R&D along 4 axes, modeling, study of fundamental scintillation mechanisms, defects and radiation damage, production technologies. This work, conducted in part by the Crystal Clear collaboration [7], has open the way to the engineering of scintillators as well as the exploitation of the impressive potential of nano-photonics and the introduction of new production technologies.

5.1. Engineering of scintillators

Through a detailed modeling of the band structure of several hosts it has been possible to define the density of states in the conduction and valence bands of several scintillators and to better understand the mechanisms of charge and energy transfer in these materials in the presence of different doping ions. Some examples of scintillator engineering are given here. A detailed review can be found in [15].

5.1.1. Alkali-halides

It is interesting to notice that alkali-halide scintillators such as thallium doped sodium iodide and cesium iodide NaI:Tl and CsI:Tl, the most widely used scintillators in medical imaging since more than 60 years [16,17], are still the subject of intense research and modeling of their respective scintillation mechanism, influence of point defects, carrier migration, exciton energy and charge transfer, etc. As a result better understanding and extended knowledge were gained and impressive performance gains were realized.

A striking example is given by Csi:Tl, an excellent and efficient scintillator but suffering from an important afterglow. In order to suppress the afterglow the idea to co-dope the crystal with aliovalent ions (namely divalent ions) has been proposed. The point here is to open to the charge carriers trapped by the shallow traps associated with thallium ions a non-radiative recombination channel to compete with the slow radiative one responsible for the afterglow. An alternative approach is to create deep traps, acting as scavengers for the above-mentioned shallow traps. Several attempts have been made, in particular with Eu^{2+}, Sm^{2+}, but Yb^{2+} co-doping has resulted in a substantial increase of the light yield with a reported value of 90,000 ph/MeV, an energy resolution of 7.9% for 511 keV γ-rays and an impressive suppression of the afterglow at the level of 0.035% after 80 ms [18].

5.1.2. Rare-earth halides

Since the discovery of lanthanum bromide, $LaBr_3$, in 2001 [19] an impressive R&D effort has concentrated on the rare-earth halide family, motivated by a very high light yield and unprecedented energy resolution in the domain of energy relevant for medical imaging applications (see Table 3). Because of their exceptional energy resolution these crystals are ideal for precise low energy spectroscopy, in particular for homeland security and astrophysics applications. However a relatively low density and a high hygroscopicity make them less attractive for PET scanners. They could however find application in scintigraphy camera if their price could be made competitive with NaI:Tl and CsI:Tl.

The reason for the high light yield of these scintillators, and in particular of $LaBr_3$ is a small bandgap of 5.6 eV, still large enough to prevent thermal delocalization of electrons and holes trapped by the 5d excited state or 4f fundamental state of the trivalent rare-earth activator ion in the conduction or valence band respectively.

Table 3
Optical and scintillation properties of rare-earth halide crystals. Reproduced from [15].

Crystal	Density (g/cm^3)	Bandgap (eV)	Ce^{3+} (Eu^{2+}) 5d–4f emission (nm)	Ce^{3+} (Eu^{2+}) 4f–5d absorption (nm)	Ce (Eu) conc. (mole%)	Scintillation decay time (ns)	Light yield (10^3 ph/MeV)	Energy resolution @ 662 keV (%)
$LaCl_3$:Ce	3.86	7	337, 358	243, 250, 263, 274, 281	10	24 (60%)	50	3.1
$LaBr_3$:Ce	5.03	5.6	355, 390	260, 270, 284, 299, 308	5	16	70	2.6
LuI_3:Ce	5.6	n.r.	475, 520	~300, 390, 419	0.5.	< 50 (50%)	42 (0.5 μs), 51 (10 μs)	4.7
					2		58 (0.5 μs), 71 (10 μs)	
$CeBr_3$	5.18	n.r.	370, 390	n.r.	100	17	60	4.1
$CeBr_3$:Sr	5.18	n.r.	370, 390	n.r.	99.5	17	55	3
$LaBr_3$:Ce,Sr	5.03	5.6	355, 390	260, 270, 284, 299, 308	5	18 (78%) 82–2500 (22%)	77	2.0
SrI_2:Eu	4.6	5.5	435	n.r.	5	600–1600	80–120	2.6–3.7
$CsBa_2I_5$:Eu	4.8	n.r.	435	n.r.	7	48 (1%), 383 (6%), 1500 (68%), 9900 (25%)	80–97	3.8

An interesting and successful attempt of scintillator engineering has been experienced on $LaBr_3$ and $CeBr_3$, where it was shown that strontium co-doping was substantially improving the energy resolution of these scintillators to 3%@662 keV for $CeBr_3$ and even 2%@662 keV [20] for $LaBr_3$. The reason is a strong reduction of the low energy non-proportionality as can be seen in Fig. 4. By introducing a shallow electron trap divalent strontium ions contribute to decrease the free electron density in the lattice and consequently the rate of Auger non-radiative recombination, which is one of the recognized cause of non-proportionality.

5.1.3. Oxyde compounds

Among oxyde scintillators garnet materials attract a lot of interest because of their excellent performance in particular for laser applications [21]. Moreover crystals like YAG and LuAG have been extensively studied and are relatively easy to grow. More recently it was shown that multicomponent garnets such as gadolinum gallium aluminium garnet ($Gd_3Ga_3Al_2O_{12}$:Ce, also called GGAG) exhibit a much higher light yield, in the range of 60,000 ph/MeV. The reason is related to a strong decrease of the concentration of traps below the bottom of the conduction band, preventing ionization-induced quenching of the excited 5d level of the Ce^{3+} activator ion.

An important and recently discovered point is related to the positive role of the tetravalent Ce^{4+} ions in some oxyde materials. By opening a channel of fast radiative recombination they can efficiently compete with electron traps for capturing electrons from the conduction band. These ions will be quickly reduced to excited Ce^{3+} ions by this electron capture and give rise to the standard cerium emission. Different co-doping strategies have been developed to stabilize the 4+ ionization state of cerium in several compounds for this purpose. The use of divalent doping such as Ca^{2+} or Mg^{2+} has proven to be efficient in reducing the decay time of GGAG [22], an effect of particular interest for the development of time-of-flight PET scanners.

The positive role of Ce^{4+} ions has also been observed in LSO [23] and more generally in the whole orthosilicate family. In these crystals the tetravalent state of cerium is stabilized by Ca^{2+} co-doping. This fast radiative decay channel complements the standard Ce^{3+} one and contributes to significantly reduce both the rise time and the decay time. Recent measurements made at CERN on LSO:Ce and LSO:Ce, Ca have shown an improvement from 70 ps to 21 ps for the rise time and from 40 ns to 33 ns for the decay time respectively [24].

Table 4 summarizes the properties of the most extensively used or studied oxide scintillators for medical applications.

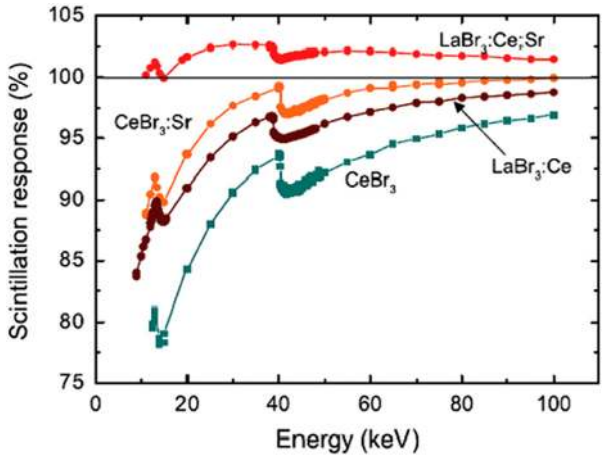

Fig. 4. X-ray response curves from Ce and Ce, Sr co-doped $LaBr_3$ and $CeBr_3$ crystals. The improvement in proportionality induced by Sr doping in clearly visible, particularly for $LaBr_3$:Ce, Sr. Picture extracted for Ref. [19].

5.2. Ultrafast timing

The search and development of scintillators in the last decades has been mainly oriented towards higher light yield and better proportionality in order to improve the energy resolution and shorter decay time to cope with higher event rates and better identify and reject scattering events. Recent years have seen the emergence of fast timing capability as a new requirement, mainly driven by time-of-flight positron emission tomography (TOF-PET) applications. Indeed TOF techniques in PET are expected to bring a number of advantages, such as a significant improvement of the image signal to noise ratio and a strong reduction of image artifacts in case of incomplete angular coverage and for tomographic reconstruction. For this purpose a coincidence time resolution in the range of 100 ps FWHM is desired, which would correspond to 1.5 cm along the line of response (LOR) between the two detectors in coincidence. It is to be noticed that a first generation of TOF-PET scanners is now commercially available with a timing resolution of about 600 ps. Prototype systems are being developed with a resolution approaching 200 ps [25]. Despite being a significant improvement over standard PET cameras, this precision does not yet allow a direct 3-D reconstruction of a PET image, which is the ultimate goal. This however requires a CTR of about 10 ps for a spatial resolution of 1.5 mm along the LOR. Such a precision would allow an on-line image reconstruction of unprecedented S/N ratio

Table 4
Optical and scintillation properties of most commonly used oxide scintillators. Reproduced from [14].

Crystal	Density (g/cm^3)	Bandgap (eV)	Ce^{3+} (Pr^{3+}) $5d^1$–$4f$ emission (nm)	Ce^{3+} (Pr^{3+}) $4f$–$5d^1$absorption (nm)	Ce (Pr) conc. (mole %)	Scintillation decay time (ns)	Light yield (10^3 ph/MeV)	Energy resolution @ 662 keV (%)
YAG:Ce	4.56	7.5	550	458	0.2	90–100	28–30	6–7
LuAG:Ce	6.67	7.8	525	448	0.15	55–65	24–26	6–7
GGAG:Ce	6.2	6.5–6.7	540	440–450	0.3	90–170	50–58	4.2–5.2
LuAG:Pr	6.67	7.8	308	284	0.1	20–22	18–20	4.6–5
LuYAG:Pr	6.2–6.5	7.7	310	286	0.1	20–22	27–33	4.4–6
YAP:Ce	5.35	8.2	365	303	0.2	19–25	22–25	4.5–5.5
YAP:Pr	5.35	8.2	247	215	0.1	8–10	6–12	11–13
LYSO:Ce, Ca	7.2	7.2	400	357	0.1	30–35	30–32	8–9
(Cd,La)PS: Ce	5.4–5.7	6.6–6.8	365–370	338	0.3	45–50	36–41	5–6

eliminating the time consuming iterative or back-projection algorithms.

Achieving ltimate time resolution on scintillator-based detectors requires a parallel effort on the light production mechanisms, light transport optimization to reduce the travel time spread of the photons on their way to the photodetector, on the photoconversion system as well as on the readout electronics [26]. The timing performance of a scintillator is directly related to the density of scintillation photons produced in a time frame corresponding to the targeted time resolution. A high light yield (LY) and a short decay time (τ_d) are mandatory as in first approximation the initial photon density is given by LY/τ_d. But this is an approximation only as scintillators are also characterized by a rise time (τ_r), which delays the emission of first produced photons, increases their time jitter and reduces accordingly the time resolution of the scintillator.

The radiative transition on the activator ion or on the intrinsic luminescent center only takes place after a complex relaxation mechanism of the primary electron–hole pairs that can last several nanoseconds. The process being stochastics large statistical fluctuations are therefore induced for the generation of the first scintillation photons at the origin of the observed rise time. There is therefore an intrinsic limit to the time resolution that can be achieved by a scintillator. It is related to the time fluctuations in the relaxation process that can be estimated to be of the order of 100 ps.

For a better sub-100 ps time resolution mechanisms involving the production of prompt photons need to be considered. Cerenkov emission and cross-luminescent materials can offer a solution. However the production of Cerenkov photons from the recoil electrons resulting from a 511 keV γ conversion is very weak, of the order of 20 photons in crystals like LSO, LuAP and GSO. Moreover these photons are preferentially emitted in the UV part of the spectrum, where the optical transmittance and the photodetector quantum efficiency are generally low. The same applies for cross-luminescent materials characterized by a reasonably fast emission (600 ps for BaF_2) but in the 100–250 nm spectral range. There are however some transient phenomena in the relaxation process that can be possibly exploited for the generation of prompt photons. From this point of view an interesting phase of the relaxation mechanism is the thermalization step when the hot electrons and holes have passed the ionization threshold. The coupling to acoustic and optical phonons in the lattice is the source of hot intraband luminescence (HIBL) that could be exploited to obtain a time tag for the interaction of ionizing radiation with a precision in the picosecond range [27]. This emission is rather weak but extremely fast (sub-ps) and is characterized by a flat spectrum in the visible for the electron-induced HIBL in the conduction band with an onset in the near

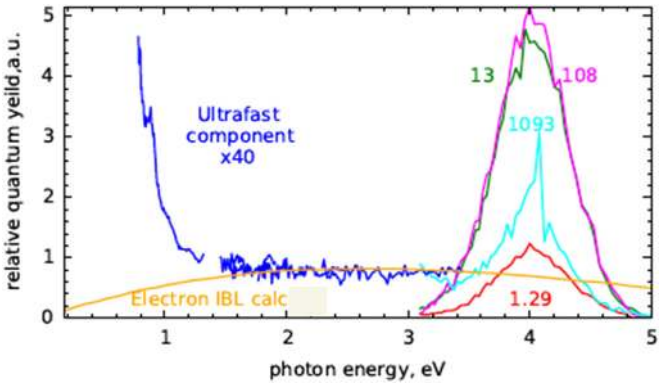

Fig. 5. Spectrum of sub-ns component of cathodoluminscence of CsI at $T=295$ °K (x40 curve, blue). Components of main CsI emission (decay time in ns). Model of e-IBL (almost flat over the whole spectrum, orange). From Ref. [29]. (For interpretation of the references to color in this figure legend, the reader is referred to the web version of this article.)

infrared attributed to the hole HIBL in the valence band. An example of such a spectrum is given in Fig. 5. From recent tests on LYSO, BGO, CeF_3 and PWO a preliminary estimation of the HIBL yield could be made and is at the level of a few tens of photons per MeV [28]. Work is going on to see if a proper engineering of the scintillator in order to produce a non-uniform density of states in the conduction and/or the valence band could yield to a more intense HIBL emission. It must be noted however that a few hundreds of prompt photons would be enough to significantly improve the time resolution of scintillators like LSO.

Another way to produce prompt photons is to develop heterostructures based on a combination of standard scintillators (such as LSO or LYSO) and nanocrystals. Nanocrystals have gained considerable attention over the last two decades because of their excellent fluorescence properties. In such systems quantum confinement offers very attractive properties, among which a very high quatum efficiency and ultrafast decay time. Moreover they have a broadband absorption and narrow emission, enhanced stability compared to organic dyes, and the fluorescence is essentially tunable from the UV, over the visible, to the near-infrared spectral range (300–3000 nm) by nanocrystal size and material composition.

A novel route toward the realization of ultrafast timing resolution is possible with the use of colloidal CdSe nanosheets (CQwells) [30], a new class of two-dimensional materials. CQwells are solution-processed analogs to epitaxial quantum wells (Qwells), but because they are synthesized in solution, they can be deposited on any substrate with any geometrical configuration.

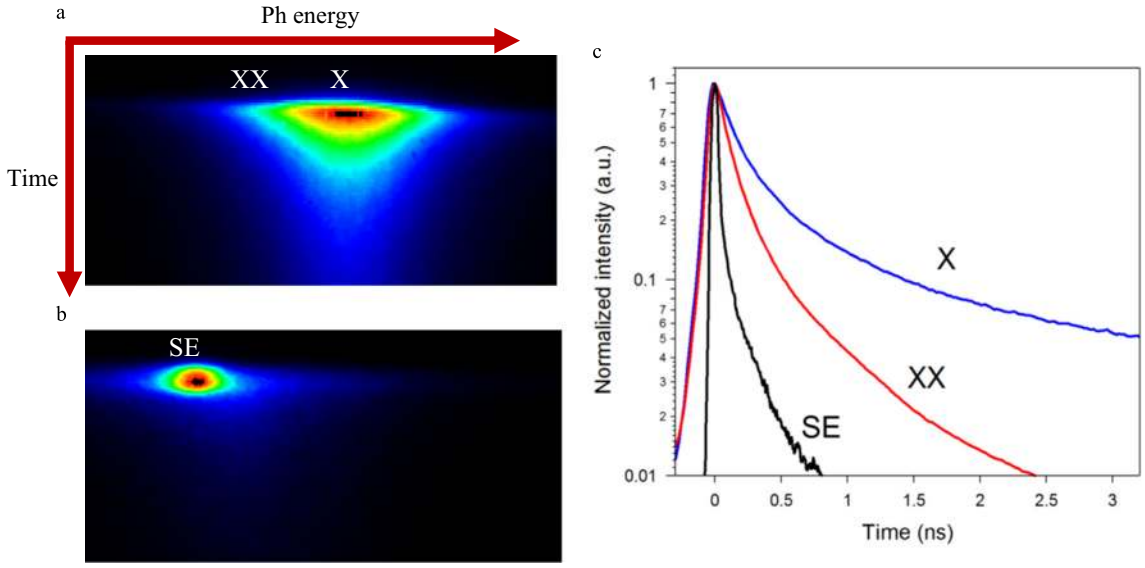

Fig. 6. Time-resolved spectral decay under femtosecond excitation (a) Streak image showing the spectral decay of exciton (X) and biexciton (XX) emission from CdSe CQwells. (b) Stimulated emission at an ultralow excitation fluence of $F_0=6\ \mu J/cm^2$, with characteristic spectral narrowing and lifetime shortening.

Further, a large dielectric mismatch between the inorganic CdSe CQwells and the surrounding organic environment results in much stronger quantum confinement than in epitaxial Qwells. This mismatch combined with very little dielectric screening due to the 1.5 nm CQwell thickness results in strongly enhanced exciton and biexciton binding energies of 132 and 30 meV, respectively, making both populations stable at room temperature.

The strong electron and hole confinement in one dimension and free motion in the plane has several important consequences, including strict momentum conservations rules (in contrast to quantum dots) and a giant oscillator strength transition. Momentum conservation in CQwells limits the available states for Auger transitions, reducing the recombination rate of this nonradiative channel. In addition to the enhanced exciton and biexciton binding energies, a giant oscillator transition results in radiative lifetimes that are significantly shorter than in bulk CdSe (~400 and ~100 ps, respectively). All of these properties contribute to the ultralow threshold stimulated emission (or superluminescence) with sub-ps decay time that has been observed with these CQwells [31] (Fig. 6). Such systems could find interesting application in ultrafast X-ray imaging as well as for providing a fast time tag in γ imaging if used in hetero-structures in combination with dense scintillators like LSO with a structuration dimension of the order of the recoil electron range, as suggested in Ref. [32].

5.3. Production technologies

The choice of the crystal growth technologies used for the production of crystals for medical imaging applications is driven by a cost effective strategy based on the growth of crystal ingots as big as possible (500 kg ingots for NaI:Tl) followed by a mechanical processing phase, i.e. cutting and polishing to the desired shapes for the different applications. However two important cost drivers remain, which are related on one hand to the high melting temperature of some crystals, in particular oxides (2050 °C for LSO) and to the increasing impact of the mechanical processing cost when higher crystal granularity is required to improve the spatial resolution. These limitations can be overcome taking advantage of recent advances in crystal production technologies.

5.3.1. MPD

The recently developed pulling-down technology from a shape-controlled capillary die gives the possibility to produce elongated crystals with dimensions that are not accessible using traditional cutting and polishing of bulk crystals grown by the more standard Czochralski or Bridgeman methods. The size of the melting zone in the pulling-down technique is up to one order of magnitude smaller than that observed in the Czochralski method. Therefore, it is believed that the pulling-down process can be considered as a good way to achieve stationary pulling conditions and can facilitate the growth process. This approach has a number of advantages, such as growing the crystal in shape (round, oval, square, rectangular, hexagonal), very fast (several millimeters per minute instead of millimeters per hour for standard crystal growth), simultaneous multifiber pulling, increased activator doping concentration even for those with high segregation coefficient, etc. Excellent quality BGO, YAG and LSO fibers have been grown with a length of up to 2 m and a diameter between 0.3 and 3 mm (see Fig. 7). Some other materials are being studied, in particular from the very interesting perovskite family: YAP and LuAP.

5.3.2. Ceramics

The impressive progress in nanotechnologies is opening new perspectives for the production of pre-reacted raw materials of excellent quality with a very small distribution of he grain sizes. With these new materials transparent ceramics of heavy scintillators can be produced (Fig. 8), with the advantage over standard crystal growth techniques to be much more cost effective: not only the scintillator can be produced to its final shape, saving on the cost of mechanical processing, but also the temperature for sintering is usually much lower than for standard crystal growth.

The R&D for the production of transparent ceramics has started in the 1990's driven by a high demand for low cost garnet production for laser applications. Applied to scintillators the R&D concentrated on YAG and LuAG ceramics. The progress in the optical transmittance of these ceramics has been such that it became as good as for bulk Czokralski grown materials. Moreover the synthesis process below the melting temperature prevents the exchange of cations from the different raw material oxides and the formation of antisite defects, which are at the origin of traps and of a reduction of scintillation efficiency in Czokralski grown crystals.

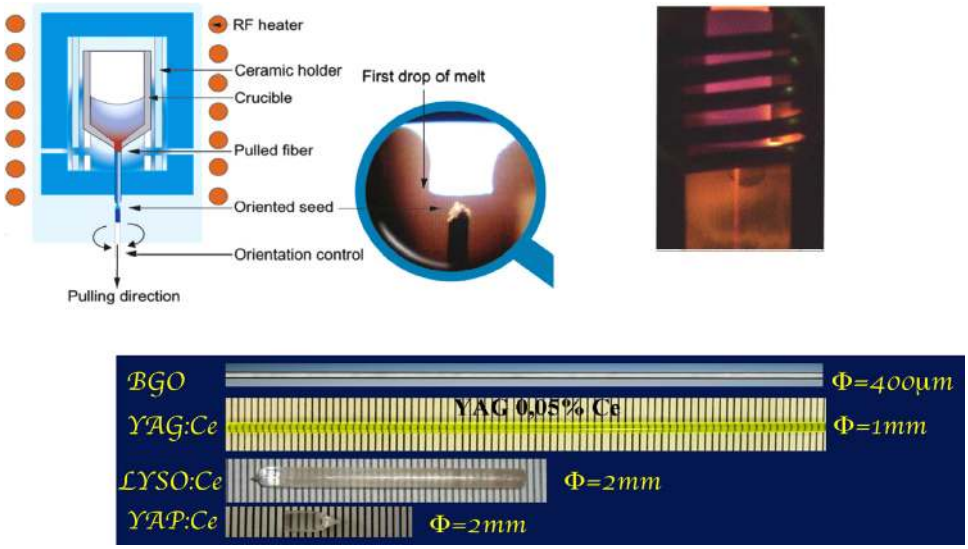

Fig. 7. The micro-pulling down crystal growth technology (Courtesy Fibercryst).

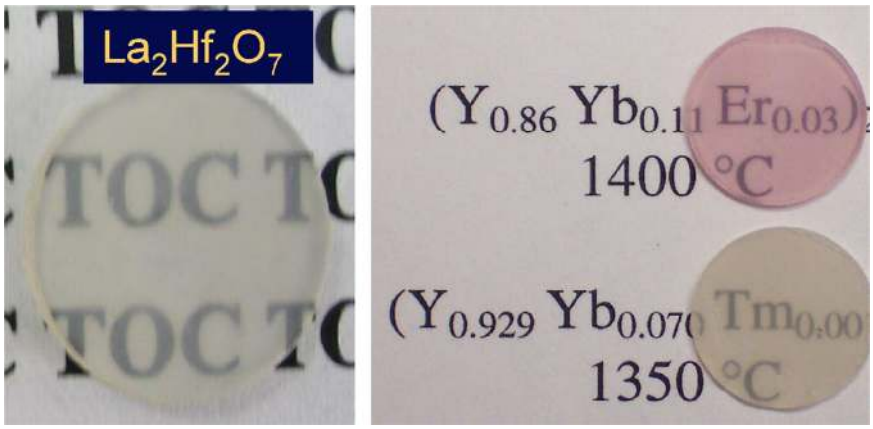

Fig. 8. Transparent ceramics of different heavy scintillators prepared with pre-reacted nanopowders.

As a consequence recent garnet ceramics show a superior light yield as Czokralski grown crystals [33].

6. Conclusion

With the steady increase of the medical imaging practice partly related o the strong emergence of personalized medicine the demand for precise, highly sensitive and quantitative molecular imaging methods is becoming every day more important. The pressure is particularly high on scintillating crystals, which are at the heart of nuclear medicine imaging (PET and SPECT). Fortunately the multidisciplinary community working on scintillator science has joined and coordinated its efforts in the last two decades to better understand the fundamental mechanisms underlying the different scintillation processes and to optimize and develop crystal production technologies.

The fundamental limitations in terms of light yield, energy resolution and timing resolution are now better understood and it becomes possible to engineer scintillating materials to optimize or customize their performance for specific applications. A number of co-doping strategies have been developed to suppress the negative influence of non-radiative traps at the origin of a loss of scintillation efficiency or afterglow. In some cases the introduction of new traps at some well-chosen energy levels could help reducing afterglow or even enhancing the light yield by increasing the probability of exciton trapping by luminescent centers. The rapid progress in nano-technologies open a number of ways to explore the fantastic domain of nano-photonics with unprecedented potential in terms of efficiency, fast timing and photon management, such as tuning emission wavelength.

Finally the crystal production technology is also a domain where research and development is very active. The micro-pulling-down techniques allow to grow meter long scintillating crystal fibers with different section shapes. Transparent ceramics are also rapidly developing with scintillating properties sometimes better than standard bulk material.

Acknowledgments

The author would like to dedicate this paper to late Prof. Vitaly Mikhailin, who has always been a vivid source of inspiration for his research. He would also like to warmly thank all his colleagues from the Crystal Clear collaboration and from the SCINT conference community for continuous and passionate exchange of views during the last 25 years. A particular tribute is paid to Andrei Belsky, Steve Derenzo, Christophe Dujardin, William Moses, Martin Nikl, Christian Pedrini, Andrei Vasiliev, Marvin Weber, Richard Williams and many others.

This work has been done with the support from CERN and from the European Research Council for the ERC Advanced Grant TICAL #338953.

References

[1] D. Deych, J. Dobbs, S. Marcovici, B. Tuval, Cadmium tungstate detector for computed temograhy, in: P. Dorenbos, C.W.E. van Eijk (Eds.), Inorganic Scintillators and Their Application, Delft University Press, Delft, 1996, pp. 36–39.
[2] S. Gundackeret al., JINST 2013, 1748-0221 8 P07014, http://dx.doi.org/10.1088/1748-0221/8/07/P07014, and S. Gundacker, P. Lecoq et al., private communication.
[3] W. Kostler, A. Winnacker, W. Rossner, B.C. Grabmaier, Journal of Physics and Chemistry of Solids 56 (1993) 907.
[4] C. Greskovich, D. Cusano, D. Hoffman, R. Riedner, American Ceramic Society Bulletin 71 (1992) 1120.
[5] E. Gorokhova, V. Demidenko, O. Khristich, S. Mikhrin, P. Rodnyi, Journal of Optical Technology 70 (2003) 693.
[6] Y. Ji, J. Shi, Journal of Materials Research 20 (2005) 567.
[7] Crystal Clear Collaboration, RD18, CERN/DRDC/P27/91-15.
[8] C.L. Melcher, Nuclear Instruments and Methods in Physics Research A 314 (1992) 212.
[9] C. Kuntner et al., Advances in the scintillation performance of LuYAP:Ce single crystals, in: Proceedings of the 7th conference on Inorganic Scintillators and their Use in Scientific and Industrial Applications, Valencia, Spain, September 2003, Nuclear Instruments and Methods in Physics Research A, vol. 537, 2005, pp. 295–301.
[10] T. Usui, et al., IEEE Transactions on Nuclear Science NS54 (1) (2007) 19.
[11] C.M. Pepin, et al., IEEE Nuclear Science Symposium Conference Record (2007) 2292.
[12] C. Kuntner, et al., Nuclear Instruments and Methods A 493 (2002) 131.
[13] W.W. Moses, IEEE Transactions on Nuclear Science NS59 (5) (2012) 2038.
[14] M.S. Alekhin, et al., Journal of Luminescence 145 (2014) 518.
[15] M. Nikl, A. Yoshikawa, Advanced Optical Materials 3 (2015) 463.
[16] R. Hofstadter, Physical Review 75 (1949) 796.
[17] W. van Sciver, R. Hofstadter, Physical Review 84 (1951) 1062.
[18] Y. Yu, M. Nikl, et al., CrystEngComm 16 (2014) 3312.
[19] E.V.D. van Loef, P. Dorenbos, C.W.E. van Eijk, K.W. Kraemer, H.U. Guedel, Applied Physics Letters 79 (2001) 1573.
[20] F. G.A., et al., NIMA 735 (2014) 655.
[21] M. Nikl, et al., Progress in Crystal Growth and Characterization of Materials 59 (2013) 47.
[22] K. Kamada, et al., Optical Materials 41 (2015) 63, http://dx.doi.org/10.1016/j.optmat.2014.10.008.
[23] H.E. Rothfuss, C.L. Melcher, et al., IEEE Transactions on Nuclear Science NS56 (2009) 958.
[24] S. Gundackeret al., to be published in the Proceedings of SCINT2015 conference, Berkeley, June 2015.
[25] N. Aubry, et al., JINST 8 (2013) C04002, http://dx.doi.org/10.1088/1748-0221/8/04/C04002.
[26] P. Lecoq, European Reserach Council ERC Advanced Grant TICAL #338953.
[27] P. Lecoq, M. Korzik, A. Vasiliev, IEEE Transactions on Nuclear Sciences NS61 (1) (2014) 229.
[28] S. Omelkovet al., to be published in the Proceedings of SCINT2015 Conference, Berkeley, June 2015.
[29] D. Vaisburd, Russian Physics Journal 40 (1997) 1037.
[30] J.Q. Grim, et al., Nature Nanotechnology 9 (2014) 891.
[31] J.Q. Grim, P. Lecoqet al., Proceedings of SCINT2015, Berkeley, 7–12 June, 2015, to be published in IEEE Transactions on Nuclear Sciences.
[32] P. Lecoq, IEEE Nuclear Science Symposium Conference Record N07-1 (2008) 680.
[33] M. Nikl, et al., in: J.J. Roa Rovira, M.S. Rubi (Eds.), Recent Advances in Ceramic Materials Research, Nova Science Publishers, chapter 6, Hauppauge NY 11788-3619 United States of America, 2013, pp. 127–176 , ISBN 978–1–62417–729–3.